been developed under some gross approximations, the calculated results have shown good agreement with experimental data using theoretical small-signal IMPATT characteristics. The circuit model developed is not restricted to IMPATT devices and should be applicable to similar waveguide circuits used for other solid-state devices.

Acknowledgment

The authors wish to thank R. S. Ying and E. M. Nakaji for providing the IMPATT devices, Dr. R. L. Bernick for providing Fig. 8, and Dr. T. A. Midford for many helpful discussions and encouragement during the course of this work.

References

[1] H. J. Kuno and D. L. English, "Nonlinear and large-signal characteristics of millimeter-wave IMPATT amplifiers," *IEEE Trans. Microwave Theory Tech.*, vol. MTT-210, pp. 703–706, Nov. 1973.
[2] ——, "Millimeter-wave IMPATT power amplifier/combiner," this issue, pp. 758–767.
[3] E. Yamashita and J. R. Baird, "Theory of a tunnel diode oscillator in a microwave structure," *Proc. IEEE*, vol. 54, April 1966.
[4] D. C. Hanson and J. E. Rowe, "Microwave circuit characteristics of bulk GaAs oscillators," *IEEE Trans. Electron Devices*, vol. ED-14, pp. 469–476, Sept. 1967.
[5] L. Infeld, "The impedance of a rectangular waveguide with a thin antenna," *Can. J. Res. Sect. A*, vol. 27A, pp. 109–129, July 1949.
[6] L. Lewin, "A contribution to the theory of probes in waveguides," *Inst. Elec. Eng. Mono. 259R*, pp. 109–116, Oct. 1957.
[7] R. L. Eisenhart and P. J. Kahn, "Theoretical and experimental analysis of a waveguide mounting structure," *IEEE Trans. Microwave Theory Tech.*, vol. MTT-19, pp. 706–719, August 1971.
[8] J. A. Bradshaw, "Scattering from a round metal post and gap," *IEEE Trans. Microwave Theory Tech.*, vol. MTT-21, pp. 313–322, May 1973.
[9] J. Schwinger and D. S. Saxon, *Discontinuities in Waveguides*. New York: Gordon and Breach Science Publishers, 1968.
[10] L. Lewin, *Advanced Theory of Waveguides*. London: Iliffe, 1951.
[11] R. E. Collin, *Field Theory of Guided Waves*. New York: McGraw-Hill, 1960.
[12] B. C. DeLoach, "A new microwave measurement technique to characterize diodes and an 800-GC cutoff frequency varactor at zero volt bias," *IEEE Trans. Microwave Theory Tech.*, vol. MTT-12, pp. 15–20, Jan. 1964.
[13] T. Misawa, "Negative resistance in p-n junction under avalanche breakdown conditions, Pts. I and II," *IEEE Trans. Electron Devices*, vol. ED-13, pp. 137–151, Jan. 1966.
[14] W. N. Grant, "Electron and hole ionization rates in epitaxial silicon at high electric fields," *Solid-State Electronics*, vol. 16, pp. 1189–1203, 1973.
[15] D. L. Scharfetter and H. K. Gummel, "Large signal analysis of silicon Read diode oscillator," *IEEE Trans. Electron Devices*, vol. ED-16, pp. 64–67, Jan. 1969.

Millimeter-Wave IMPATT Power Amplifier/Combiner

H. J. KUNO, SENIOR MEMBER, IEEE, AND DAVID L. ENGLISH, ASSOCIATE MEMBER, IEEE

Abstract—**The development of a two-stage millimeter-wave IMPATT power amplifier/combiner is described herein. The driver stage consists of a two-diode hybrid-coupled amplifier and the output stage consists of a four-diode combiner (a pair of hybrid-coupled amplifiers). An output power of 1 W was achieved with a 22-dB small-signal gain and a 6-GHz bandwidth in the 60-GHz range. Design considerations and experimental data are presented in detail.**

Introduction

THE APPLICATION of IMPATT devices in millimeter-wave systems has gained great importance in recent years. It has been demonstrated that IMPATT oscillators and amplifiers can be used effectively for millimeter-wave power generation and amplification [1]–[7]. It is of great interest to combine a number of diodes to achieve high output power. In the microwave frequency range various power combining approaches have been tried [8]–[14]. However, the same technique cannot readily be applied directly at millimeter-wave frequencies. This paper describes the development of a millimeter-wave IMPATT power amplifier/combiner with which a continuous-wave (CW) output power of 1 W was achieved with a 6-GHz small-signal bandwidth in the 60-GHz range.

The hybrid-coupled power amplifier/combiner, as applied to the millimeter-wave range, offers the following advantages over other approaches.

1) The power-impedance limitation of multidevice operation in a single cavity is removed. However, as will be shown in the next section, other considerations limit the number of devices which may be efficiently combined.

2) Since the hybrid coupler provides isolation between the individual amplifier cavities, instability problems associated with multidevice operation in a single cavity are minimized.

3) Ferrite circulators are not required if 90° hybrids are used.

4) Since hybrid couplers provide broad-band characteristics (BW = 10 GHz at 60 GHz), broad amplifier bandwidth can be achieved.

5) Since each amplifier cavity can be tuned individually, amplifiers can be well matched.

Manuscript received February 27, 1976; revised May 21, 1976. This work was supported in part by the Air Force Avionics Laboratory, Air Force Systems Command, U.S. Air Force, Wright-Patterson Air Force Base, OH.

The authors are with Hughes Aircraft Company, Torrance, CA.

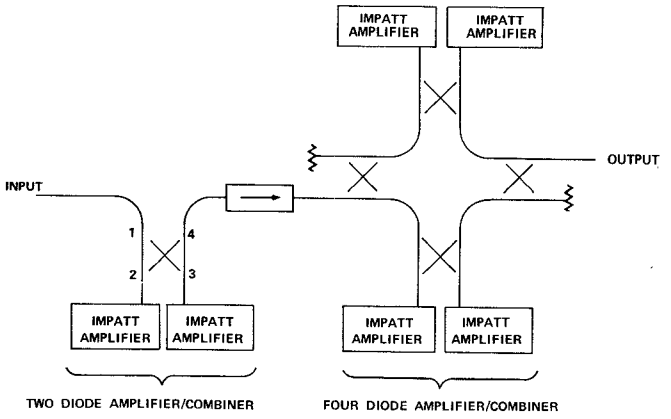

Fig. 1. Block diagram of a two-stage amplifier/combiner utilizing hybrid-coupled amplifiers.

We have demonstrated the feasibility of hybrid-coupled amplifiers by successfully and efficiently combining the output powers of four single-diode amplifiers.

Power Amplifier/Combiner Design Considerations

Referring to Fig. 1, the principle of the hybrid-coupled IMPATT amplifier operation can be described in the following way. When input power is applied to port 1, the power will be evenly coupled to ports 2 and 3, and port 4 is isolated from port 1. If ports 2 and 3 are terminated by a pair of balanced loads such as matched reflection amplifiers, a signal applied at port 1 will be amplified and reflected from ports 2 and 3. The reflected waves will be added at port 4, but canceled at port 1 due to the phase relationship between the two reflected waves. Thus the power applied to port 1 will be amplified and accumulated at port 4. If the amplifiers are unbalanced either in amplitude or phase, a portion of the amplified signal will be coupled back to the input port and lost in the input termination. This principle can be extended to a larger number of amplifiers.

Shown in Fig. 1 is a schematic diagram of the two-stage IMPATT power amplifier/combiner. The first stage combines two amplifiers and the second combines four. We had originally planned on using a single-diode circulator-coupled amplifier as the driver stage. However, present technology limits the bandwidth of low-loss V band circulators to approximately 3 GHz. Thus, in order to take full advantage of the broad-band high-power characteristics of the hybrid-coupled amplifier, we used one as a driver stage as well as two in the output stage. Two IMPATT amplifiers are combined in the driver stage and four are combined in the output stage. A wide-band isolator is used between stages.

Let us analyze the power combining efficiency and the expected output power for the hybrid-coupled amplifiers. Power combining with symmetrical four-port hybrid couplers is achieved by dividing the input signal power, routing it to single-diode amplifiers through several parallel branches, and then summing the amplified powers of the several branches into one output port. The power division and summation functions are performed by the hybrid couplers. Because of the symmetry requirement, the number of individual IMPATT diodes allowed is

$$N_d = 2^k$$

and the number of hybrid couplers necessary when no circulators are used is

$$N_h = 3 \cdot 2^{(k-1)} - 2$$

where k is the combining number, which can be any integer. It will be shown below that the primary factor in the reduction of the combining efficiency from ideal is the insertion loss of the hybrids. Thus, assuming that individual amplifiers are ideally matched both in amplitude and phase, we find that the net combiner gain is given by

$$G_t = L_h^{-2} G_i$$

and that the net output power

$$P_t = 2^k L_h^{-k} P_i$$

where L_h is the insertion loss of the hybrid coupler (per path), G_i is the individual diode gain, and P_i is the individual amplifier output power. The combining efficiency is given by

$$N_c = L_h^{-k}$$

and the total added power is

$$P_{\text{add}} = (2^k L_h^{-k}) \left(1 - \frac{L_h^{2k}}{G_i}\right) P_i.$$

Thus we see that there are limits on the number of diodes which can be combined with hybrid couplers, because the gain, combining efficiency, and added power approach zero with increasing combining number when losses in the hybrid couplers are taken into consideration, i.e., $L_h > 1$. A realistic point of diminishing returns may be defined as the point where the net gain is 3 dB, i.e., the added power equals the input power.

The insertion losses of the short-slot hybrid couplers used in the present power combiner were measured to be 0.5 dB per path over a 7-GHz bandwidth. Also, as will be shown in the next section, the best single-diode amplifiers produce 325 mW of output power at a gain of 6 dB. Using these numbers for a four-diode combiner, we get a combining efficiency of 79 percent, a net gain of 3.95 dB, and a total output power of 1.05 W. These numbers are very close to the performance which was actually achieved with our four-diode combiner.

In addition to the insertion losses of the hybrid couplers, phase and amplitude matching of the individual amplifiers are also important factors that determine the upper limit of the number of diodes that can be combined by hybrid couplers. It will be shown later how IMPATT amplifiers can be matched in both small-signal and large-signal characteristics.

Another degradation factor in hybrid-coupled combiners is the loss of the isolators which must be used between stages and at the input and output ports. It is necessary to use wide-band isolators for this purpose because of the very large IMPATT-amplifier bandwidths. Such isolators have

a 0.9-dB insertion loss. If one isolator is included, the combiner gain is reduced to 3.05 dB. Thus combining more than four diodes would lead to the point of diminishing returns.

IMPATT Diode and Amplifier Circuit

The output-power capability of IMPATT diodes ultimately determines the upper limit of the achievable output power from the amplifier/combiner. The diodes used are p^+-n-n^+-type single-drift Si IMPATT diodes. For the 60-GHz range, we found that diodes with 14–16-V breakdown voltages yielded the best combination of the maximum output power and gain–bandwidth product [1].

It has been shown that an IMPATT diode operated as a reflection amplifier and driven to a 3-dB saturated gain can generate as much added power as it does when operated as an optimally loaded oscillator [2]. For a 6-dB saturated gain, the total amplifier output power is approximately 1.25 times that of the optimally loaded oscillator. The diodes used in the amplifier/combiner typically yielded 250–300 mW as oscillators when biased at a junction temperature of 260°C. (At this junction temperature a mean time between failures (MTBF) greater than 10^4 h can be expected.)

A cross-sectional view of the basic amplifier circuit [1] is shown in Fig. 2. It consists of a reduced-height waveguide cavity where there is a mounted diode, an adjustable coaxial section, a movable short, and a quarter-wavelength impedance transformer section. The microwave characteristics of the circuit can be represented by a simplified equivalent circuit, shown in Fig. 3. This circuit provides two degrees of freedom in tuning: a series tuning element provided by the adjustable coaxial section and a parallel tuning element provided by the movable short. In this way, both the real and imaginary components of the load impedance can be matched to those of the device to achieve optimum performance over a specified frequency range [1].

In addition to the electrical characteristics of the circuit, it is also important to provide low thermal resistance between the diode and the heat sink in order to remove heat generated in the diode. In the circuit shown in Fig. 2, the packaged diode is directly mounted onto the circuit. The thermal resistances of typical diodes mounted in the circuit for operation in the 60-GHz range have been measured to be approximately 35°C/W for single-drift diodes and 30°C/W for double-drift diodes.

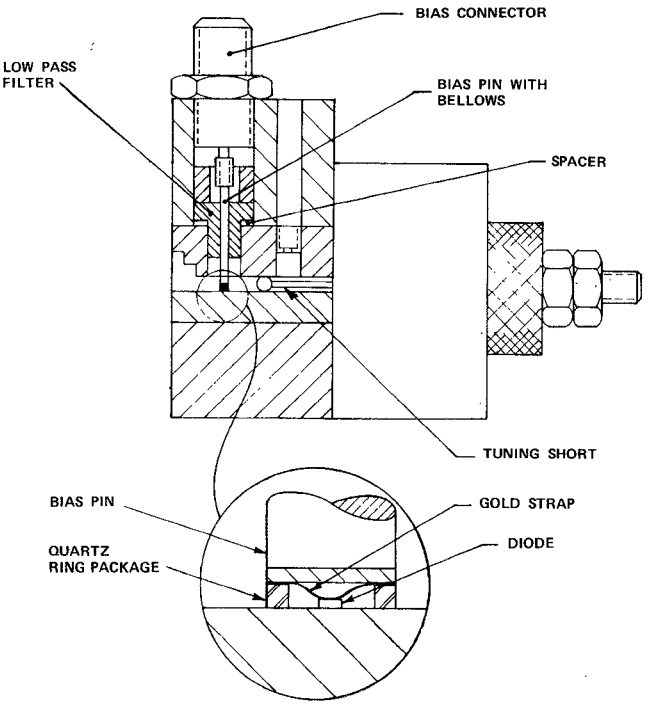

Fig. 2. Cross section of a reduced-height waveguide IMPATT oscillator/amplifier circuit.

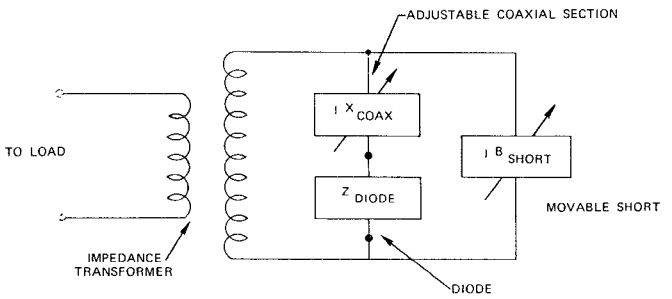

Fig. 3. Equivalent circuit of millimeter-wave IMPATT amplifier circuit.

Hybrid-Coupled Amplifier/Combiner

For IMPATT amplifier combining, either 90° short-slot hybrids or 180° matched magic-tee hybrids may be used. Magic-tee's have a lower insertion loss but also a narrower voltage standing-wave ratio (VSWR) bandwidth, while 90° hybrids have the advantage that the input and output ports of the hybrid-coupled amplifier are separate, which allows the use of ferrite isolators instead of circulators. This is advantageous because isolators can be built with full waveguide bandwidths in V band while circulators have maximum bandwidths of 3 GHz in the 60-GHz range. In addition, circulators have high out-of-band VSWR's, which cause stability problems in reflection amplifiers. For these reasons, we used short-slot 90° hybrid couplers for the amplifier/combiner.

The hybrids have capacitive tuning slugs centered on the slot. For amplifier applications, it was found desirable to adjust the slugs for a minimum VSWR over the largest possible bandwidth. The hybrid couplers were tuned to give a VSWR less than 1.15 over a 9-GHz bandwidth. The two-way insertion loss was then measured to be less than 1.3 dB over the same 9-GHz band and less than 1 dB over a 7-GHz bandwidth. The isolation was greater than 15 dB over the 7-GHz bandwidth.

In a hybrid-coupled amplifier/combiner, the amplifier pair must be matched in both amplitude and phase. By matching small-signal bandpass curves of the two amplifiers, a good bandpass characteristic can be obtained from the hybrid-

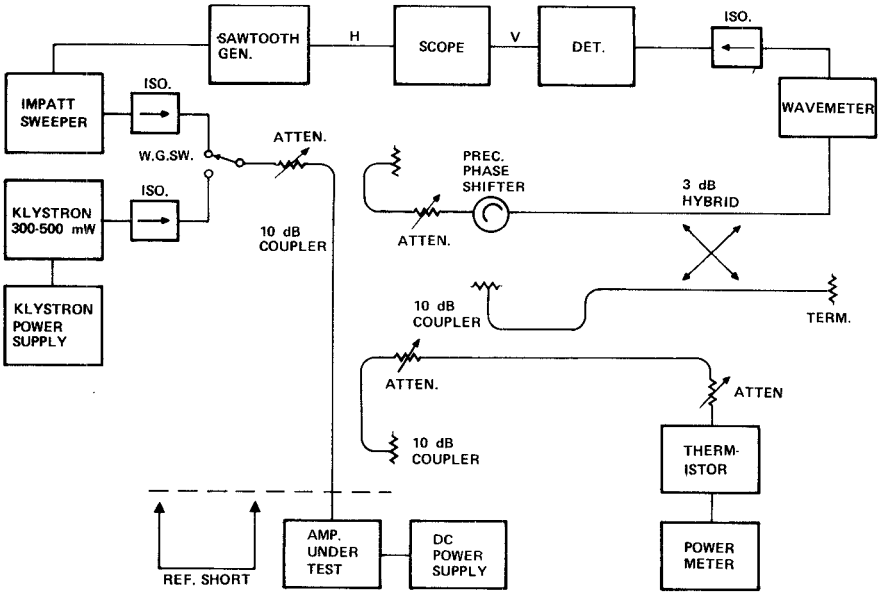

Fig. 4. Block diagram of large-signal power and phase test setup.

coupled amplifier. However, when driven to large-signal levels, the hybrid-coupled amplifiers often do not yield the output power expected from the individual diode power transfer curves. Thus it is important to match amplifier characteristics at large-signal levels to achieve high output power from hybrid-coupled amplifier/combiner units.

The large-signal power, gain, and phase characteristics of six high-power broad-band single-diode reflection amplifiers were measured. Since high-level swept-frequency power was not available, the measurements were taken point by point at five discrete frequencies of a 5-GHz range in the phase-bridge test set shown schematically in Fig. 4. The diodes were individually mounted in an amplifier cavity with tuning elements adjusted for a smooth broad-band response at small-signal levels with gains of 10–14 dB. After this initial tuning, the tuning elements were locked in place for the remaining power and phase measurements. The dc bias current of each diode was set to a value which gave a junction temperature of approximately 260°C. A phase reference was obtained from an amplifier cavity with the bias hole plugged, and the tuning short set to the position where the IMPATT diode would normally be mounted.

Typical data for one diode from these measurements are shown in Fig. 5. Since only five discrete frequencies were used, the graphs of gain versus frequency at high input power and phase versus frequency show the general trend rather than the fine structure. These data have shown that, in general, the saturated output power decreases with increasing frequency by as much as 2.8 dB in going from 57.5 to 62.5 GHz. This is due to the lowering of the resonant frequency at high signal levels. At a constant input power level below the saturation point (40–50 mW, for example), the power falloff with frequency is not nearly as severe; and the output power of all of the diodes are flat to within ± 0.6 dB over the full 5-GHz frequency range. The data have also shown that diodes of the same breakdown voltage and junction capacitance from the same production run have remarkably uniform power and phase characteristics over the 5-GHz bandwidth. For such diodes, if the small-signal bandpass characteristics and power transfer curves at a single frequency are similar, the amplifiers are likely to be well matched for large-signal power and phase characteristics over a wide frequency range. Four diodes, which were selected in the manner described, were found to have large-signal gains matched to within 0.4 dB and large-signal phase shifts matched to within 25° over the full 5-GHz bandwidth. It can be shown that mismatches of this order contribute only a few tenths of a decibel to the combining losses of a hybrid-coupled amplifier. Thus, for hybrid-coupled amplifier/combiner units, diodes having similar breakdown voltages and junction capacitances should be selected.

The deviation from a linear phase slope and the AM-to-PM conversion can also be found from the curves of Fig. 5. The deviation from linearity for all cases is largest at the low-frequency end of the band, but improves considerably as the input-signal frequency moves up beyond 59 GHz. The AM-to-PM conversion factor is largest at the low-frequency end for intermediate power levels but, at higher power levels, is largest near the center of the band.

In fabricating hybrid-coupled amplifiers, pairs of diodes were first selected on the basis of the detailed power and phase characteristics of individual diodes. The amplifiers were then retuned slightly so as to obtain the smoothest bandpass response from the hybrid-coupled pair.

A number of hybrid-coupled amplifiers were constructed and their bandpass and power transfer characteristics were evaluated. The amplifier test setup shown in Fig. 4 was used for evaluating hybrid-coupled amplifiers, except that the directional coupler was removed because the hybrid-coupled

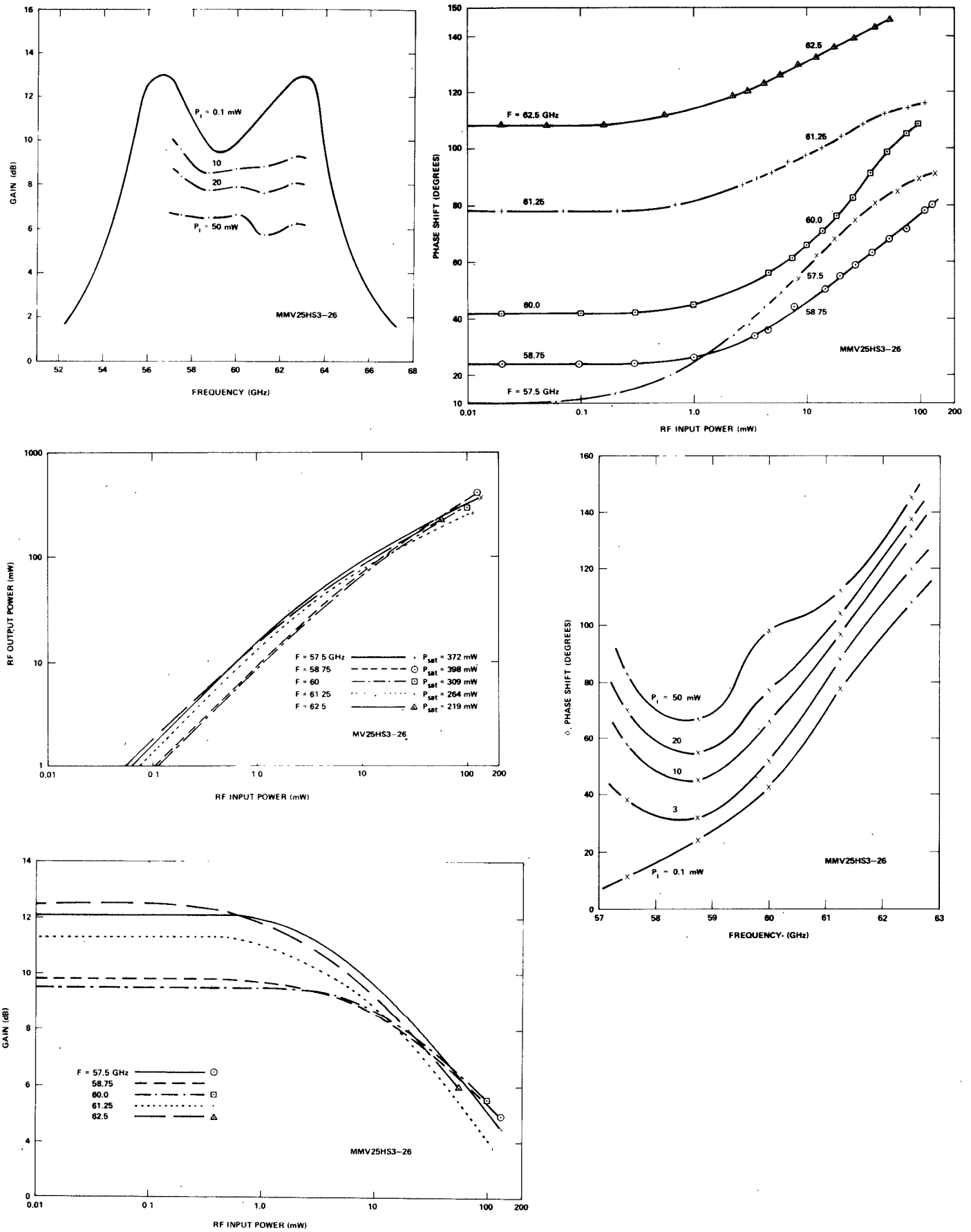

Fig. 5. Large-signal bandpass, power, gain, and phase characteristics of a typical high-power single-diode IMPATT amplifier.

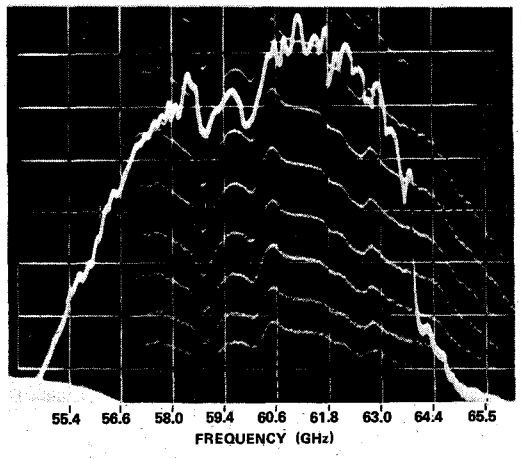

GAIN CALIBRATION LINES 2 dB/STEP. TOP CALIBRATION LINE FOR G=14 dB.

(a)

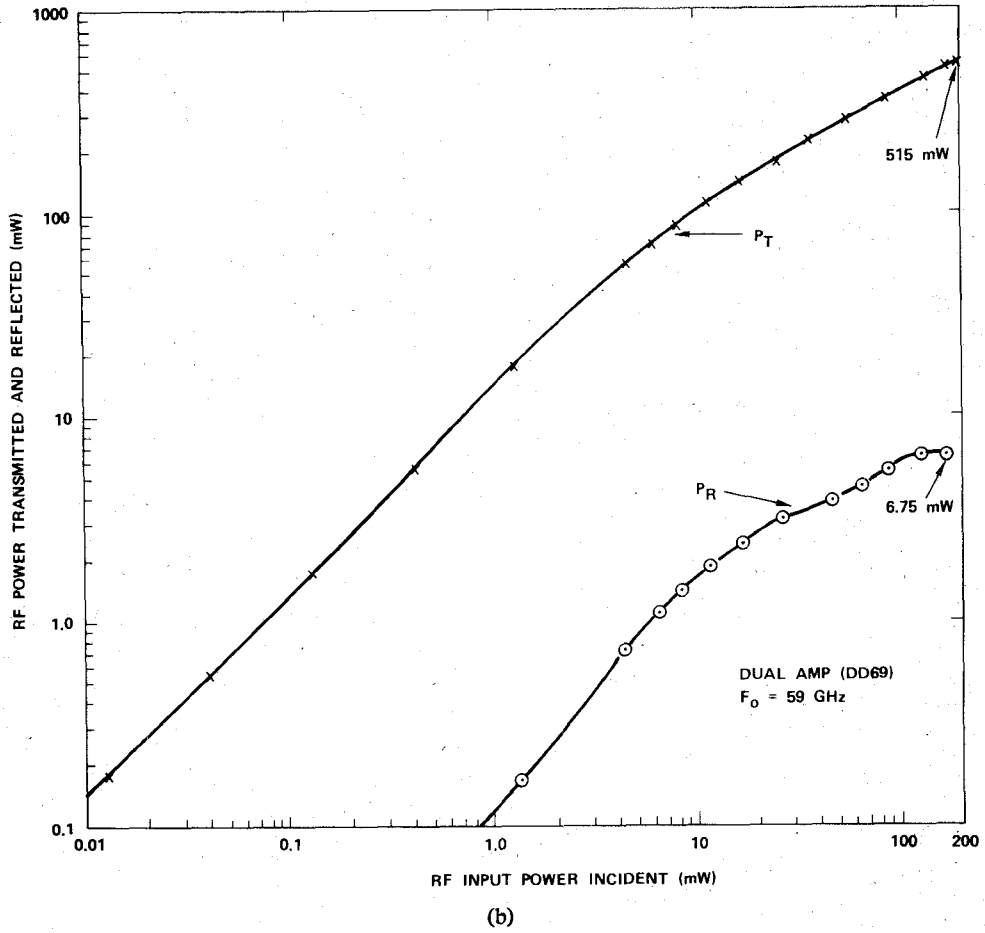

(b)

Fig. 6. (a) Small-signal bandpass. (b) Large-signal power transfer characteristics of a hybrid-coupled IMPATT amplifier.

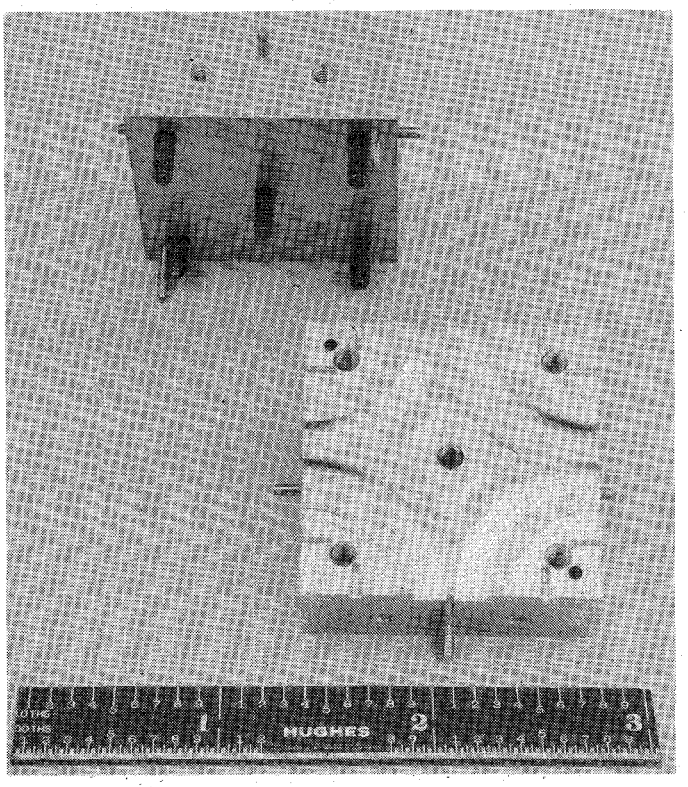

Fig. 7. Precision four-way waveguide adaptor for connecting four hybrids in the four-diode combiner/amplifier.

amplifiers have separate input and output ports. Typical small-signal bandpass and large-signal power transfer characteristics of the two-diode hybrid-coupled amplifiers are given in Fig. 6.

The quality of match between diodes in a hybrid-coupled amplifier is indicated by the ratio of transmitted to reflected powers. Ratios ranging from 15 to 19 dB have been measured. The best hybrid-coupled amplifier constructed produced 600 mW of output power at a saturated gain of 6 dB and a small-signal bandwidth of 8 GHz.

Four-Diode Power Combiner/Amplifier

By combining a pair of hybrid-coupled amplifiers, we can construct a four-diode power combiner/amplifier. In order to minimize size and reduce phase mismatches among the signal paths of the combiner, a miniature four-way waveguide adaptor such as shown in Fig. 7 was fabricated. This unit was used to connect two hybrid-coupled amplifiers and two additional hybrid couplers as shown in Fig. 1.

The four-diode combiner output stage was formed with the two separate hybrid-coupled amplifiers. The measured bandpass characteristics and the power transfer curves of the four-diode combiner are shown in Fig. 8.

By referring to the characteristics of the individual diodes which comprise the combiner, it was determined that the combining efficiency and output power were degraded primarily by the hybrid-coupler losses rather than diode mismatches. The combiner produced an output power at 59 GHz of 1.075 W with a 3.6-dB gain. At an output of 1 W the gain was 4.3 dB. The 3-dB bandwidth was approximately 7 GHz and the gain ripple was ± 0.7 dB over a 6-GHz band. The dc to RF (power added) conversion efficiency was 2.3 percent.

For good stability in a circulator-coupled reflection amplifier, the return loss of the circulator should be much greater than the gain of the amplifier when connected to a flat load. A similar criterion, in which the combined effects of reflections at both input and output ports are taken into account, is valid for hybrid-coupled amplifiers. The isolators used had VSWR's which peaked at 1.3 (a return loss of 17.7 dB) at certain frequencies. When this is compared with peak amplifier gains of 12 dB, it can be expected that the isolators introduce ripples in the bandpass characteristics. The four-diode combiner was not nearly as sensitive to load reflections as were the two-diode hybrid-coupled amplifiers and did not, in fact, oscillate when either its input or output port was left open. This is partly due to the terminations at the two unused ports, which absorb that portion of the power due to amplitude and phase mismatches between the individual diode amplifiers, and partly due to the losses in the hybrids. If the diode amplifiers are all well matched, no power will be absorbed by either termination.

Two-Stage Power Amplifier/Combiner

By combining a two-diode hybrid-coupled amplifier and a four-diode power amplifier/combiner, a two-stage power amplifier/combiner such as shown in Fig. 9 was constructed. For interstage isolation, a broad-band isolator was used. After the two stages were connected together no further tuning was necessary.

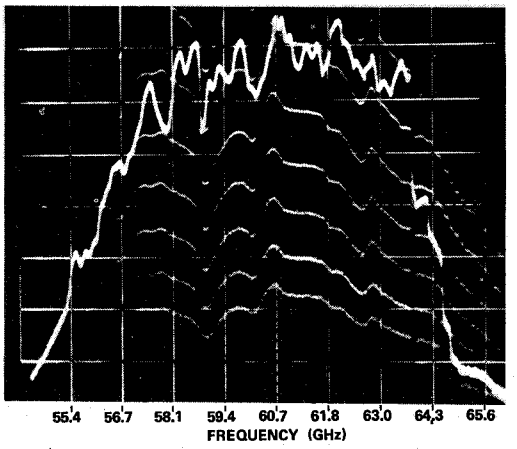

(a)

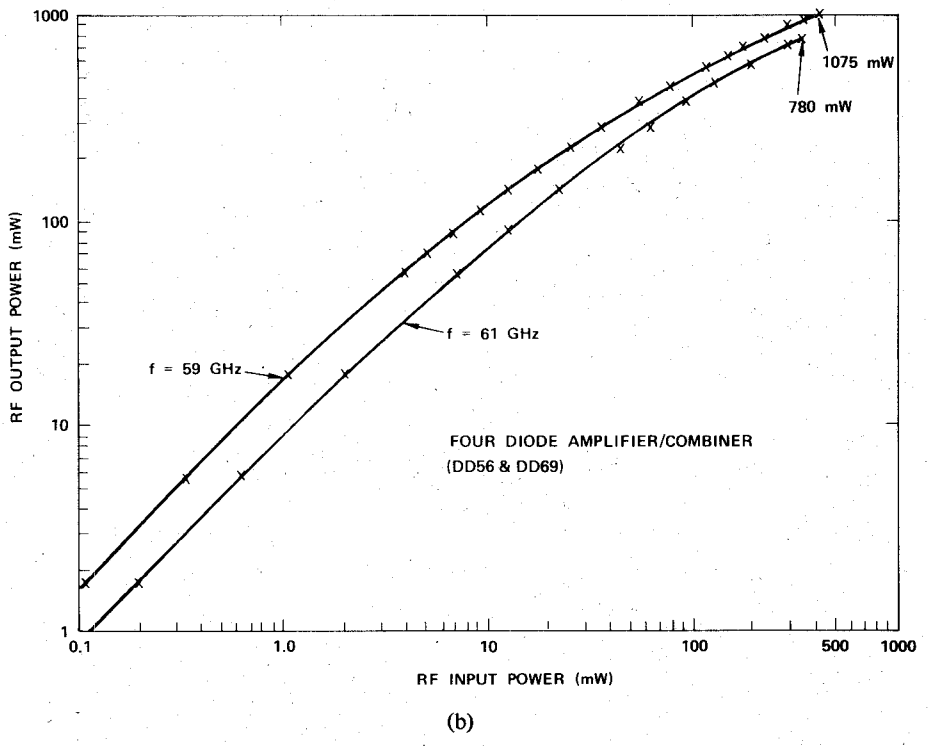

(b)

Fig. 8. (a) Small-signal bandpass. (b) Large-signal power transfer characteristics of the four-diode IMPATT amplifier/combiner.

Shown in Fig. 10 are the measured overall bandpass and power transfer characteristics of the complete two-stage amplifier/combiner. A small-signal gain of 21 dB with a 3-dB p-p ripple over a 6-GHz bandwidth was achieved. The saturated output power at 59 GHz was 0.98 W with 9 dB of gain. At the 0.5-W output level, the gain was 16 dB. The large ripple in the bandpass curve was due to the combined effects of the isolator VSWR and interaction between stages through the isolator with 30 dB of isolation.

Conclusions

A two-stage hybrid-coupled amplifier/combiner consisting of a two-diode amplifier/combiner at the first stage and a four-diode amplifier/combiner at the second stage has been developed. Output power of 1 W has been achieved, with a small-signal gain of 22 dB and a bandwidth of 6 GHz in the 60-GHz range. The amplifier/combiner unit was also operated with a high-data-rate transmitter module recently developed in our laboratory [4].

The results described in this paper have demonstrated the feasibility of efficiently combining a number of IMPATT devices at millimeter-wave frequencies to achieve high output power with broad bandwidth.

References

[1] H. J. Kuno and D. L. English, "Nonlinear and large-signal characteristics of millimeter-wave IMPATT amplifiers," *IEEE Trans. Microwave Theory Tech.*, vol. MTT-21, pp. 703–706, Nov. 1973.
[2] H. J. Kuno, "Analysis of nonlinear characteristics and transient

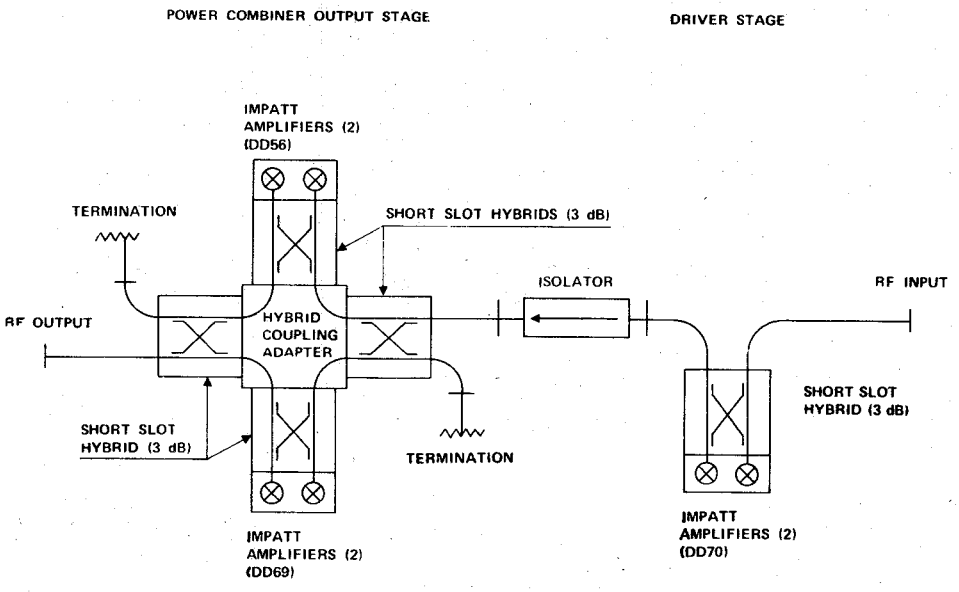

(a)

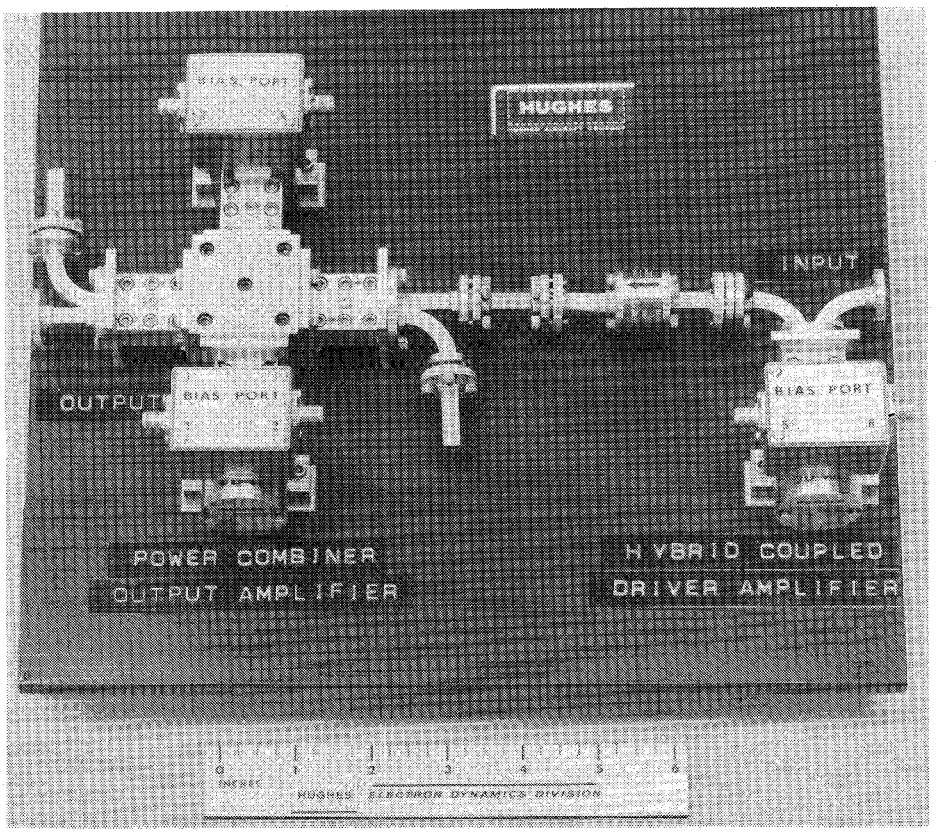

(b)

Fig. 9. (a) Block diagram. (b) Photograph of two-stage IMPATT amplifier/combiner.

response of IMPATT amplifiers," *IEEE Trans. Microwave Theory Tech.*, vol. MTT-21, pp. 694–702, Nov. 1973.
[3] H. Hayashi *et al.*, "80 GHz IMPATT amplifier," in *1974 ISSCC Digest of Technical Papers*, vol. XVII, pp. 102–103, Feb. 1974.
[4] Y. Chang, H. J. Kuno, and D. L. English, "High data-rate millimeter-wave transmitter module," *IEEE Trans. Microwave Theory Tech.*, vol. MTT-23, pp. 470–477, June 1975.
[5] K. P. Weller, R. S. Ying, and E. M. Nakaji, "Millimeter-wave 94 GHz silicon IMPATT amplifiers," in *1975 ISCC Digest of Technical Papers*, vol. XVIII, pp. 128–139, Feb. 1975.
[6] T. Miyakawa *et al.*, "Wideband tunable and highly stabilized millimeter-wave IMPATT oscillators," in *1975 IEEE-MTT Microwave Symp. Digest of Technical Papers*, pp. 222–223, May 1975.
[7] C. A. Tearle and K. R. Hearth, "IMPATT pump sideband noise and its effect on parametric amplifier noise temperature," *IEEE Trans. Microwave Theory Tech.*, vol. MTT-23, pp. 1036–1042, Dec. 1975.
[8] K. Kurokawa, "The single cavity multiple device oscillator," *IEEE Trans. Microwave Theory Tech.*, vol. MTT-19, pp. 793–801, Oct. 1971.

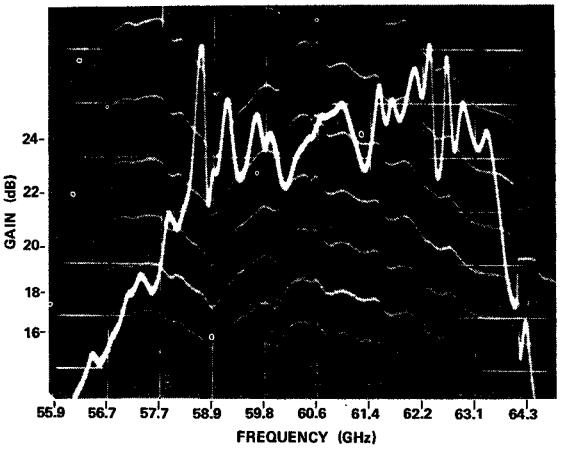

GAIN CALIBRATION LINES 2 dB/STEP. TOP CALIBRATION LINE FOR G=24 dB.

(a)

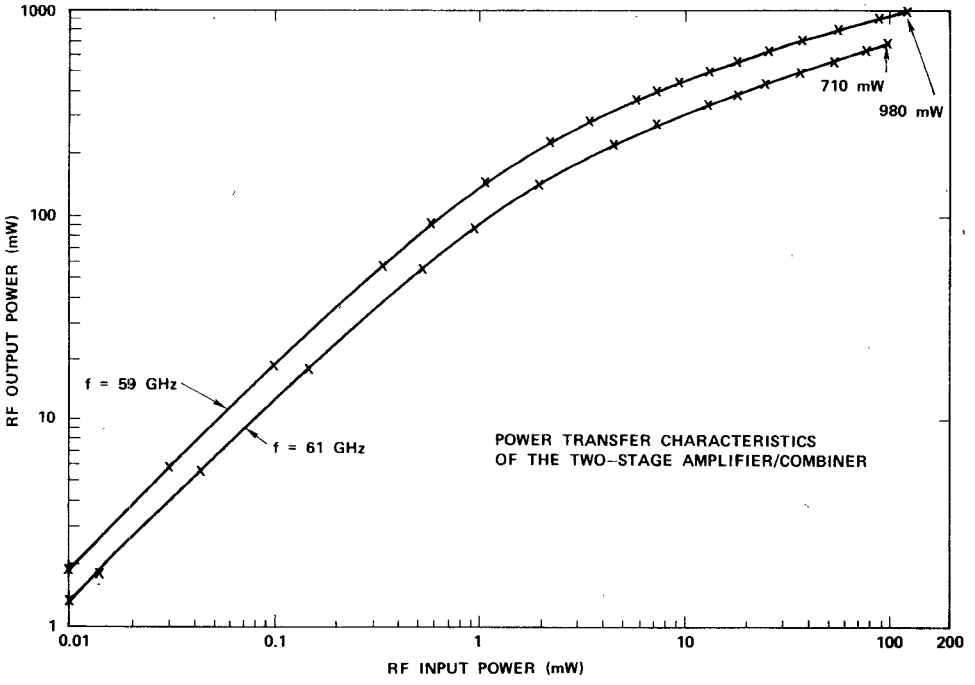

(b)

Fig. 10. (a) Small-signal bandpass. (b) Power transfer characteristics of complete two-stage IMPATT amplifier/combiner.

[9] K. Kurokawa and F. M. Magalhaes, "An *X*-band 10-watt multiple-IMPATT oscillator," *Proc. IEEE*, vol. 59, pp. 102–103, Jan. 1971.
[10] H. J. Kuno *et al.*, "Push-pull operation of transferred-electron oscillators," *Electron. Lett.*, vol. 5, pp. 178–179, May 1, 1969.
[11] M. E. Hines *et al.*, "Distributed undirectional microwave amplification," presented at the IEEE Int. Microwave Symposium, Washington, DC, May 1917.
[12] R. S. Harp and H. L. Stover, "Power combining of *X*-band IMPATT circuit modules," in *1973 ISSCC Digest of Technical Papers*, vol. XVI, pp. 118–119, Feb. 1973.
[13] R. S. Harp and K. J. Russell, "Improvements in bandwidth and frequency capability of microwave power combinatorial techniques," in *1975 ISSCC Digest of Technical Papers*, vol. XVII, pp. 94–95, Feb. 1974.
[14] K. J. Russell and R. S. Harp, "Power combiner operation with pulsed IMPATTs," in *1975 ISSCC Digest of Technical Papers*, vol. XVIII, pp. 136–137, Feb. 1975.